Title: Recovery of Holothuroidea population density, community composition and respiration activity after a deep-sea disturbance experiment

Authors and affiliations: Tanja Stratmann[1*], Ilja Voorsmit[2], Andrey Gebruk[3], Alastair Brown[4], Autun Purser[5], Yann Marcon[5,6], Andrew K. Sweetman[7], Daniel O. B. Jones[8], Dick van Oevelen[1]

[1]NIOZ Royal Netherlands Institute for Sea Research, Department of Estuarine and Delta Systems, and Utrecht University, P.O. Box 140, 4400 AC Yerseke, The Netherlands.

[2]Faculty of Mathematics and Natural Sciences, University of Groningen, P.O. Box 11103, 9700 CC Groningen, The Netherlands.

[3]P.P. Shirshov Institute of Oceanology, Russian Academy of Sciences, Nakhimovsky Pr., 36, Moscow 117997, Russia.

[4]Ocean and Earth Science, University of Southampton, National Oceanography Centre Southampton, European Way, Southampton, SO14 3ZH, United Kingdom.

[5]Deep Sea Ecology and Technology, Alfred Wegener Institute, Am Handelshafen 12, 27570 Bremerhaven, Germany.

[6]MARUM, Center for Marine Environmental Sciences, Leobener Str., 28359 Bremen, Germany.

[7]The Marine Benthic Ecology, Biogeochemistry and In-situ Technology Research Group, The Lyell Centre for Earth and Marine Science and Technology, Heriot-Watt University, Edinburgh EH14 4AS, United Kingdom.

[8]Ocean Biogeochemistry and Ecosystems, National Oceanography Centre Southampton, European Way, Southampton SO14 3ZH, United Kingdom.

*Corresponding author

23 e-mail addresses: T Stratmann: tanja.stratmann@nioz.nl, Ilja Voorsmit:
24 iljavoorsmit@gmail.com, Andrey Gebruk: agebruk@gmail.com, Alastair Brown:
25 Alastair.Brown@noc.soton.ac.uk, Autun Purser: autun.purser@awi.de, Yann Marcon:
26 ymar-con@marum.de, Andrew K. Sweetman: a.sweetman@hw.ac.uk, Daniel O. B. Jones:
27 dj1@noc.ac.uk, Dick van Oevelen: Dick.van.Oevelen@nioz.nl
28
29 Running head: Holothuroidea recovery after disturbance

1. Abstract

Mining polymetallic nodules on abyssal plains will have adverse impacts on deep-sea ecosystems, but it is largely unknown whether the impacted ecosystem will recover, and if so at what rate. In 1989 the 'DISturbance and reCOLonization' (DISCOL) experiment was conducted in the Peru Basin where the seafloor was disturbed with a plough harrow construction to explore the effect of small-scale sediment disturbance from deep-sea mining. Densities of Holothuroidea in the region were last investigated seven years post-disturbance, before nineteen years later, the DISCOL site was re-visited in 2015. An 'ocean floor observatory system' was used to photograph the seabed across ploughed and unploughed seafloor and at reference sites. The images were analyzed to determine the Holothuroidea population density and community composition, which were combined with in situ respiration measurements of individual Holothuroidea to generate a respiration budget of the study area. For the first time since the experimental disturbance, similar Holothuroidea densities were observed at the DISCOL site and at reference sites. The Holothuroidea assemblage was dominated by *Amperima* sp., *Mesothuria* sp. and *Benthodytes typica*, together contributing 46% to the Holothuroidea population density. Biomass and respiration were similar among sites, with a Holothuroidea community respiration of $5.84\times10^{-4}\pm8.74\times10^{-5}$ mmol C m^{-2} d^{-1} at reference sites. Although these results indicate recovery of Holothuroidea, extrapolations regarding recovery from deep-sea mining activities must be made with caution: results presented here are based on a relatively small-scale disturbance experiment as compared to industrial-scale nodule mining, and also only represent one taxonomic class of the megafauna.

2. Key words

Anthropogenic disturbance, manganese nodule, echinoderm, holothurian, OFOS, south-east Pacific, community composition, DISCOL

3. Introduction

Interest in mining polymetallic nodules from abyssal plains has increased substantially since the 1960s (Glasby 2000; Jones et al. 2017). Polymetallic nodules contain valuable metals such as copper, cobalt, nickel and rare earth elements (Wang and Müller 2009) and are therefore considered economically interesting resources. However, deep-sea mining activities will have negative impacts on these vulnerable deep-sea ecosystems through the removal of hard substratum (i.e. polymetallic nodules) essential for sessile (e.g. Amon et al. 2016; Vanreusel et al. 2016) and mobile (Leitner et al. 2016; Purser et al. 2016) fauna. Further negative impacts may result from the disturbance and/or removal of the upper sediment layer (Thiel and Tiefsee-Umweltschutz 2001), i.e. the habitat that contains the majority of organisms and their food sources (Danovaro et al. 1993; Danovaro et al. 1995; Haeckel et al. 2001). Sessile fauna and infauna will be removed in the mining tracks (Bluhm 2001; Borowski and Thiel 1998; Borowski 2001), and fauna in and on adjacent sediments may be blanketed by mechanically displaced sediment (Thiel and Tiefsee-Umweltschutz 2001). Re-suspended sediment and sediment plumes may smother both sessile and mobile fauna over extended areas, or potentially adversely impact filter feeding organisms (Brooke et al. 2009; Jankowski and Zielke 2001; Thiel and Tiefsee-Umweltschutz 2001).

Ecological concerns about deep-sea mining have resulted in several deep-sea experiments studying ecosystem recovery following disturbance (Jones et al. 2017). To investigate the

76 recovery from small scale disturbance experiments employing isolated individual disturbance
77 tracks, Vanreusel et al. (2016) used ROV video surveys to compare sessile and mobile metazoan
78 epifauna densities at disturbed and undisturbed sites with high and low "polymetallic nodule"
79 coverage in the Clarion-Clipperton Zone (CCZ, central Pacific). The mobile metazoan epifauna
80 in a 20-year-old experimental mining track at a nodule-free site comprised mainly Holothuroidea
81 and Ophiuroidea (1,500 ind. ha^{-1}), whereas the density at the reference site was substantially
82 higher (3,000 ind. ha^{-1}). In contrast, the same study showed that mobile metazoan epifauna at a
83 nodule-rich site in another, 37-year-old mining track in the CCZ consisted exclusively of
84 Echinoidea (1,000 ind. ha^{-1}) and had a 70% lower mobile epifauna density than the reference
85 site, where Holothuroidea and Ophiuroidea were also present.
86
87 The most extensively studied and largest-scale disturbance experiment conducted to date is the
88 'DISturbance and reCOLonization experiment' (DISCOL) in the Peru Basin. This experiment
89 was conducted in a 10.8 km^2 circular area, DISCOL Disturbance Area or 'DEA' in short, which
90 was ploughed 78 times on diametric courses in 1989 to mimic a small-scale deep-sea mining
91 disturbance event (Bluhm 2001; Foell et al. 1990; Foell et al. 1992). The DEA can be considered
92 'small-scale' in comparison to commercial mining as the 10.8 km^2 represent between 1.4 and
93 3.6% of the area projected to be disturbed by one individual mining operation per year (Smith et
94 al. 2008). The imposed disturbance occurred on two levels: 1) direct impacts inside 'plough
95 tracks' where polymetallic nodules were ploughed into the sediment (~22% of DEA) and 2)
96 indirect impacts from plume exposure associated with the ploughing outside plough tracks (~70-
97 75% of the DEA; Bluhm and Thiel 1996; Thiel and Schriever 1989). Four sites, each

98 approximately 4 km away from the DEA served as reference areas as they were considered to be
99 outside the area of plume influence.
100
101 Biological investigations were conducted inside the disturbance tracks, outside the tracks and at
102 the reference sites prior to the DISCOL disturbance (reference sites; DISCOL 1/1 cruise),
103 immediately following DISCOL disturbance (inside and outside tracks; DISCOL 1/2 cruise) and
104 half a year (DISCOL 2 cruise), three (DISCOL 3 cruise), and seven years (ECOBENT cruise)
105 post DISCOL disturbance (Bluhm 2001) to assess ecosystem recovery over time. The
106 disturbance experiment impacted the meio-, macro- and megafaunal size classes of the benthic
107 community, but the magnitude of disturbance differed markedly among size classes and
108 functional groups. For example, the abundance of meiofaunal harpacticoids was approximately
109 20% lower at the disturbed sites compared to the undisturbed sites immediately following the
110 DISCOL disturbance, a difference that persisted up to seven years after the DISCOL disturbance
111 (Ahnert and Schriever 2001). In contrast, total macrofauna abundance at the disturbed sites was
112 66% lower than at the undisturbed sites immediately following the DISCOL disturbance, but was
113 similar between disturbed and undisturbed sites three years after the DISCOL disturbance
114 (Borowski 2001). Sessile megafauna, such as Cnidaria, Crinoidea and Ascidiacea, was virtually
115 absent from disturbed sites following ploughing, and did not recover to pre-disturbance densities
116 during the subsequent seven years (Bluhm 2001). Their slow recovery is likely a result of the
117 removal of hard substratum from the seafloor (Vanreusel et al. 2016). Total megafaunal densities
118 were significantly lower in the disturbed sites directly after the DISCOL disturbance, half a year
119 after and seven years after the DISCOL disturbance, but not significantly different three years
120 after the DISCOL disturbance (Bluhm 2001). Holothuroidea, the dominant taxa of mobile

megafauna, remained reduced at disturbed sites (75 ± 50 ind. ha^{-1}) when compared with densities observed at undisturbed sites (169 ± 79 ind. ha^{-1}) seven years after the DISCOL disturbance (Bluhm 2001), though the difference was not statistically significant because of the large variability within the data.

These deposit-feeding Holothuroidea are a key component of abyssal benthic communities as they engage in key ecosystem functions of the deep sea, such as modifying the quality of the organic matter of the sediment (Smallwood et al. 1999), processing of fresh phytodetritus (FitzGeorge-Balfour et al. 2010; Bett et al. 2001), and mineralization through nutrient regeneration or respiration (Thurber et al. 2014). Holothurians make a contribution to mineralization as they were estimated to respire between 1 and 6% of the particulate organic carbon flux per year on Pacific and Atlantic abyssal plains (Ruhl et al. 2014). Many holothurian species are large in comparison to other abyssal benthic invertebrates and can therefore be counted and identified from images with comparative ease (Durden et al. 2016). Holothuroidea are also mobile, with some species moving >100 cm h^{-1} over the seafloor (Jamieson et al. 2011) and some species having the capacity to swim (Miller and Pawson 1990; Rogacheva et al. 2012). Holothuroidea can respond to fresh phytodetritus deposition events with large-scale recruitment within a year (Billett et al. 2010). One would therefore expect that Holothuroidea may recover in regions of disturbed seafloor comparatively quickly.

In this study, we assessed Holothuroidea population density and community composition twenty-six years after the initial disturbance at the DISCOL area, by determining abundances from high-resolution photos taken of the seafloor both within and outside plough tracks, and at reference sites

144 south and southeast of the DEA. The results of this abundance estimation were then combined
145 with *in-situ* respiration rate measurements to identify any differences in respiratory activity of
146 Holothuroidea at the various sites. These data were compared with earlier Holothuroidea
147 population density data to investigate a) whether the Holothuroidea assemblages differed between
148 disturbed, undisturbed and reference areas, b) whether Holothuroidea population densities had
149 recovered after 26 years, and c) whether Holothuroidea respiration rates differed between sites.
150 The mechanisms underlying the observed recovery dynamics are discussed and considered in the
151 context of future mining operations.
152
153 **4. Methods**
154 4.1 Study site
155 The seafloor in the Peru Basin in the tropical south-east Pacific Ocean is typically between 4000
156 and 4400 m deep (Wiediecke and Weber 1996), has a bottom water temperature of 2.9°C,
157 salinity of 34.6 PSU, and oxygen concentration of 145.3±1.3 (mean ± sd) µmol L^{-1} (Boetius
158 2015). Bottom water currents alternate between periods of comparatively strong (>5 cm s^{-1})
159 unidirectional currents and periods of slower (<1-3 cm s^{-1}) current flow without prevalent
160 direction (Klein et al. 1975). The DEA itself is centered on 07°04.4' S, 88°27.6' W and is
161 between 4140 and 4160 m deep (Bluhm et al. 1995). Sediment in the DEA typically consists of a
162 5 to 15 cm thick surface layer of semi-liquid, dark brown sediment (0.55 ± 0.11% organic
163 carbon) and a sublayer of consolidated greyish clay (0.70 ± 0.08% organic carbon) (Grupe et al.
164 2001; Marchig et al. 2001; Oebius et al. 2001). Surface sediments in the DEA have 18.1 ± 11.3
165 kg m^{-2} of polymetallic nodules (Marchig et al. 2001). The DEA plough tracks are still clearly
166 visible (Fig. 1) and consequently we identified three disturbance categories for the study: inside

and outside plough tracks in the DEA (hereafter referred to as disturbed site and undisturbed site respectively), and reference sites south and southeast of the DEA (hereafter referred to as reference site) (Fig. 1).

4.2 Assessment of Holothuroidea assemblage

A high-resolution digital camera (CANON EOS 5D Mark III, modified for underwater applications by iSiTEC) on the towed Ocean Floor Observation System (OFOS) was used to photograph the seafloor. The OFOS was deployed from the RV Sonne during cruise SO242-2 (chief scientist: Prof. Dr. Antje Boetius) and towed 1.5 m above the seafloor at a speed of approximately 0.5 knots, photographing the seafloor every 10 s (~5.5 m^2 seafloor per image) (Purser et al. 2016). In contrast, during previous DISCOL cruises (from directly following to seven years after the DISCOL disturbance), the OFOS was equipped with analog still-photo cameras (DISCOL 1/1, DISCOL 1/2 and DISCOL 2 cruises: Benthos 377 camera; DISCOL 3 and ECOBENT cruises: Photosea 5000 camera; Bluhm et al. 1995; Schriever et al. 1996). For these deployments, the system was towed approximately 3 m above the seafloor and the photographs were taken selectively by scientists (Bluhm and Gebruk 1999; Jones et al. 2017). For this study the OFOS was deployed four times at the DEA (Fig. 1 and table 1), where a total of 3760 usable (neither under- nor overexposed, correct altitude and without suspended sediment obscuration) pictures were taken. Images were classified as ‘disturbed site’ when plough tracks were visible (1838 photos) and otherwise classified as ‘undisturbed site’ (1922 photos; Table 1). The OFOS was also deployed four times for this study at reference sites outside the DEA (Fig. 1 and table 1), where a total of 983 usable pictures were taken. Each transect was treated as a

189 replicate resulting in four replicates for each level of disturbance (i.e. disturbed, undisturbed and
190 reference site).
191 Photographs were loaded into the open-source software "Program for Annotation of Photographs
192 and Rapid Analysis (of Zillions and Zillions) of Images" (PAPARA(ZZ)I) (Marcon and Purser
193 2017). All Holothuroidea in non-overlapping pictures were first annotated by morphotype.
194 Subsequently, morphotypes were identified to family, genus, or species level by an expert deep-
195 sea Holothuroidea taxonomist (A. Gebruk). Reference was made to Bluhm and Gebruk (1999)
196 and the 'Atlas of Abyssal Megafauna Morphotypes of the Clipperton-Clarion Fracture Zone'
197 (ccfzatlas.com). In PAPARA(ZZ)I body length and body width were measured for all
198 Holothuroidea which lay straight using as reference for scaling a set of three laser points on the
199 sea floor that formed an equilaterial triangle of 0.5 m.
200
201 4.3 Assessment of total sediment community oxygen consumption and Holothuroidea
202 community respiration
203 The sediment community oxygen consumption (SCOC) was measured *in-situ* at the DISCOL
204 reference site by deploying a benthic chamber lander (KUM GmbH, Germany) that was
205 equipped with HydroFlash^{TM} O_2 (Kongsberg Maritime Contros GmbH, Germany) optodes. After
206 deployment of the lander, incubation chambers (20×20×20 cm) were slowly pushed into the
207 sediment after which the oxygen concentration inside the chambers was continuously recorded
208 over a period of three days (Boetius 2015). From the linear decrease in oxygen concentration, the
209 oxygen consumption rate was estimated.
210 Holothuroidea community respiration was calculated based on abundance (see above) and *in situ*
211 respiration rates of 13 individual Holothuroidea sampled during RV Sonne cruise 242-2 (A.

212 Brown et al. unpubl.). Briefly, the 'benthic incubation chamber system 3' (BICS3) (Hughes et al.
213 2011) was attached to the GEOMAR Ocean elevator (Linke 2010) and lowered to the seafloor.
214 Holothuroidea were collected individually with the ROV Kiel 6000 and placed individually in
215 three respiration chambers. The forth respiration chamber was kept empty as a control. After a
216 Holothuroidea was placed in a chamber, the lid was closed immediately and oxygen
217 consumption was measured over a period of at least seventy hours (84.8±14.3 h), with the empty
218 chamber being used to assess the oxygen consumption rate of bottom seawater. Afterwards, the
219 elevator platform with the BICS3 was brought to the surface, the Holothuroidea were collected
220 and body length and width of each specimen were measured.
221 For the conversion of body length and width of individual Holothuroidea annotated on the OFOS
222 photos into individual respiration rates, the body volume of the 13 Holothuroidea specimens
223 (*Amperima* sp., *Benthodytes sp.*, *Benthodytes typica*, *Mesothuria* sp., *Peniagone* sp. 2
224 (benthopelagic), *Synallactidae* gen. sp. 2) collected inside DEA was related to background-
225 corrected respiration rates (measured originally in mmol O_2 ind^{-1} d^{-1}, A. Brown et al. unpubl.),
226 but converted to mmol C ind^{-1} d^{-1} assuming a respiratory quotient of 1). The body volume of the
227 13 Holothuroidea specimens was calculated as the body length × body width^2. This formed the
228 basis of the linear regression analysis of body volume versus background-corrected respiration
229 rates for all individual organisms (respiration rate = 9.00×10^{-5} × body length × body width^2; n =
230 13, $r^2 = 0.41$, $p = <0.001$). Subsequently, body length and width measurements of Holothuroidea
231 from the OFOS pictures were converted into respiration rates following the equation given above
232 whenever the organisms laid straight. When the length could not be measured, e.g. when the
233 specimen was in a curved position, an average size for that specific morphotype was taken. The

234 respiration per unit area was calculated as the sum of individual respiration rates divided by the
235 area for which Holothuroidea abundance was determined.
236
237 4.5 Data analysis
238 For the Holothuroidea dataset after 26 years, the univariate diversity indices Shannon index *H'*
239 and Pielou index *J'* were calculated following Magurran (2013) using the 'vegan' package in *R*
240 (Oksanen et al. 2016). Analysis of similarities in assemblage composition of Holothuroidea was
241 based on square-root transformed faunal density data using the ANOSIM routine in PRIMER6
242 (Clarke and Warwick 2008). The contribution of individual morphotypes to the similarity or
243 dissimilarity between sites was calculated with the SIMPER routine in PRIMER6.
244 Differences in *H'* and *J'* indices, Holothuroidea densities, and respiration rates among
245 disturbance levels (disturbed site, undisturbed site, reference site) were tested with One-Way
246 ANOVA using the open-source software *R* (R Core Team 2016).
247 The Holothuroidea population densities were also analyzed over time (i.e. pre-disturbance -0.1,
248 0.1, 0.5, 3, 7 and 26 years post-DISCOL disturbance) at disturbed, undisturbed and reference
249 sites. The raw Holothuroidea density data from the earlier cruises were taken from Annex 2.08 in
250 Bluhm (2001) and combined with the Holothuroidea density data of the present study. This
251 resulted in an n=6 for DISCOL1/1 (reference site), n=4 and n=5 for DISCOL 1/2 (disturbed and
252 undisturbed site, respectively), n=3, n=4 and n=2 for DISCOL 2 (disturbed, undisturbed and
253 reference site, respectively), n=4, n=4 and n=3 for DISCOL 3, n=4, n=4 and n=5 for ECOBENT
254 and n=4, n=4 and n=4 for DISCOL revisited. An unweighted One-Way ANOVA on the $\log_{10}$-
255 transformed Holothuroidea density data was applied to compare differences in Holothuroidea
256 densities from disturbed, undisturbed and reference sites of the same year.

Results are expressed as mean ± standard deviation if not stated otherwise.

5. Results

5.1 Holothuroidea population density and community composition

A total of 23 different Holothuroidea morphotypes were identified from the full image set (Fig. 2). Where image quality was insufficient to identify morphotype, Holothuroidea were classified as "unknown Holothuroidea". A total of 22 morphotypes were found at the disturbed sites, including single records of *Abyssocucumis abyssorum* and *Galatheaturia* sp., 20 morphotypes at undisturbed sites, including a single record of *Benthodytes gosarsi*, and 17 morphotypes at the reference sites (Fig. 3). The most abundant species were *Amperima* sp., *Benthodytes typica* and *Mesothuria* sp. (Fig. 3 and table 2), which together contributed 46±6% to the total density. However, their ranking in species abundance varied among sites (Fig. 3).

The density of Holothuroidea did not differ among sites (ANOVA: $F_{2,9} = 0.042$, $p = 0.96$) with mean densities (ind. ha^{-1}) of 241±51 at the disturbed site, 240±40 at the undisturbed site, and 241±33 at the reference site. There were no differences in mean density of each morphotype among sites (ANOSIM: $R = 0.019$, $p = 0.39$), either. Similarity in species composition among sites was driven by *Benthodytes typica* (contribution to similarity between disturbed and undisturbed sites: 10.46% to 16.28%), *Amperima* sp. (10.49%), and the group of unknown Holothuroidea (10.28% and 10.54%). The Shannon diversity index *H'* and Pielou evenness index *J'* did not differ significantly among sites, either (ANOVA for *H'*: $F_{2,9} = 1.914$, $p = 0.20$; ANOVA for *J'*: $F_{2,9} = 2.027$, $p = 0.19$; Table 3).

5.2 Holothuroidea density changes over time

280 The holothurian mean density of 142 ± 37 ind. ha^{-1} of the pre-disturbance study in February 1989
281 dropped by 87% (18 ± 10 ind. ha^{-1}) at the disturbed site and by 39% (86 ± 31 ind. ha^{-1}) at the
282 undisturbed site immediately after the disturbance (Fig. 4; Bluhm 2001). This difference in mean
283 Holothuroidea densities between disturbed and undisturbed site 0.1 years post DISCOL
284 disturbance was statistical significant (ANOVA: $F_{1,7} = 26.23$, $p = 0.001$) and persisted until half
285 a year after the DISCOL disturbance (ANOVA: $F_{2,6} = 16.46$, $p = 0.004$) (Bluhm 2001). Three
286 years after the DISCOL disturbance, Holothuroidea mean densities at the disturbed site (99 ± 54
287 ind. ha^{-1}) were 37% of the mean densities at the undisturbed site (266 ± 200 ind. ha^{-1}; Bluhm
288 2001), but the difference between disturbance levels was not significant anymore due to a large
289 variability among the OFOS tracks (ANOVA: $F_{2,8} = 4.18$, $p = 0.06$).
290
291 5.3 Holothuroidea community respiration
292 Holothuroidea community respiration ($\times 10^{-3}$ mmol C m^{-2} d^{-1}) was not significantly different
293 among the reference sites (0.58±0.09), undisturbed (0.77±0.10) and disturbed sites (0.80±0.30)
294 (ANOVA: $F_{2,9} = 1.591$, $p = 0.256$).
295
296 **6. Discussion**
297 Deep-sea mining for polymetallic nodules will impact the benthic ecosystem in various ways
298 (Jones et al. 2017) and it is therefore vital to estimate how long it may take for ecosystems to
299 recover from the resultant seafloor disturbances (Gollner et al. 2017). Data presented here
300 demonstrate that Holothuroidea population density, community composition, and respiration
301 have recovered 26 years after a sediment disturbance event in the Peru Basin. We here discuss
302 the mechanisms involved in the recovery of Holothuroidea composition and functioning

following the experimental disturbance and consider these in the context of future deep-sea mining activities.

6.1 Holothuroidea assemblage and densities

Holothuroidea assemblages in abyssal plains are often dominated by a few species, such as *Amperima rosea*, *Oneirophanta mutabilis*, *Psychropotes longicauda* and *Pseudostichopus villosus* at the Porcupine Abyssal Plain (PAP, north-east Atlantic; Billett et al. 2001; Billett et al. 2010) or *Abyssocucumis abyssorum*, *Peniagone vitrea* and *Elpidia minutissima* at Station M in the north-east Pacific (Smith et al. 1993). The Holothuroidea assemblage in the Peru Basin therefore resembles a typical deep-sea community, where *Amperima* sp., *Benthodytes typica* and *Mesothuria* sp. comprise almost 50% of the total Holothuroidea.

A key finding of this study is that Holothuroidea density and community composition recovered from a disturbance after twenty-six years. These results are in contrast with a study on megafaunal recovery from the CCZ, where isolated individual disturbance tracks still showed reduced Holothuroidea densities up to thirty-seven years after the disturbance (Vanreusel et al. 2016). This discrepancy may be a result of various factors, including temporal variability in Holothuroidea abundance, different disturbance methods and scales, and/or differences in the food supply to the CCZ compared to the DISCOL area.

The abundance of particular mobile abyssal megafauna taxa can fluctuate inter-annually by one to three orders of magnitude (Ruhl 2007). For example, the density of the Holothuroidea *Amperima rosea* increased by more than two orders of magnitude at the Porcupine Abyssal Plain (PAP, NE Atlantic) during the famous ‘Amperima event’ (Billett et al. 2001; Billett et al. 2010), likely in response to increased food supply to the seafloor. Hence, photo transects performed at a

particular time only represent a snapshot of the megafaunal assemblage and do not show potential temporal variability. Holothuroidea abundance in a comparatively narrow and short mining track (Vanreusel et al. 2016) where the number of individual specimen observed is likely very low is especially prone to such spatial and temporal sampling bias.

Another key difference between the CCZ and DISCOL studies is the imposed disturbance method. During the DISCOL experiment the upper sediment layer was mixed in a ~2.4 km^2 area (22% of 10.8 km^2 DEA; Thiel and Schriever 1989) leaving a mosaic of dark-brown sediment and greyish clay (Fig. 1B). In contrast, the disturbance at the CCZ involved complete removal of the upper 5 cm of sediment in individual 2.5 m wide tracks (Khripounoff et al. 2006). Surface sediments in the CCZ contain about 0.48% organic carbon (per dry sediment), whereas the carbon content in sediments below 5 cm in the CCZ is only 0.35% (Khripounoff et al. 2006). Hence, food availability in the CCZ tracks were reduced which may have contributed to the lower abundances. Other potential causes could be changes in water content with sediment depth (Grupe et al. 2001), differences in sediment compactness, sediment grain size, terrain or texture of the surface sediment in the tracks. Finally, the investigated site at the north-western CCZ is more oligotrophic as compared to the DISCOL site, with a particulate organic carbon (POC) flux estimated to be 1.5 mg C_{org} m^{-2} d^{-1} (Vanreusel et al. 2016).The flux of particulate organic carbon in the Peru Basin is higher, with model estimates of 3.86 mg C_{org} m^{-2} d^{-1} (Haeckel et al. 2001). Consequently, re-establishing food availability in tracks following disturbance will likely differ between the CCZ and the Peru Basin, because of differences in disturbance method and trophic status.

6.2 Holothuroidea respiration

The total Holothuroidea respiration at the DISCOL site (0.01 mg O_2 m^{-2} d^{-1}) was comparable to, but at the lower end of the echinoderm respiration calculated for PAP (respiration range: 0.01 to 0.04 mg O_2 m^{-2} d^{-1}; Ruhl et al. 2014) and one order of magnitude lower than the absolute echinoderm respiration calculated for station M (respiration range: 0.15 to 0.65 mg O_2 m^{-2} d^{-1}; Ruhl et al. 2014). The latter difference can be attributed to the dominance of non-Holothuroidea echinoderms to the total echinoderm respiration at station M. When only the total respiration rate of the dominant species *Ophiuroidea*, *Elpidia spp*. and *Echinocrepis rostrata* (Ruhl et al. 2014) was considered, the Holothuroidea respiration at station M was in the same order of magnitude as the Peru Basin taking into account the overall higher Holothuroidea densities in the northeast Pacific than in the southeast Pacific (Ruhl 2007; Ruhl et al. 2014).

The relative contribution of Holothuroidea to the total benthic respiration depends on the supply of POC to the system (Ruhl et al. 2014). In food-limited abyssal plains such as at station M, model estimates indicated that Holothuroidea contribute between 1.44% and 2.42% to the total community respiration (Dunlop et al. 2016). In the present study, the Holothuroidea contributed even less to the total benthic respiration with an estimated 0.18% of the community respiration of 114.98±12.90 mmol O_2 m^{-2} yr^{-1}.

6.3 Holothuroidea recovery over time

Most Holothuroidea are mobile and move over the sediment or engage in swimming behavior (Kaufmann and Smith 1997; Miller and Pawson 1990; Jamieson et al. 2011; Rogacheva et al. 2012). Assuming a unidirectional movement of 10 and 65 cm h^{-1} (Kaufmann and Smith 1997), Holothuroidea would need approximately 0.66 years to cross the entire DEA, of which only 22%

was directly denuded of Holothuroidea (Thiel and Schriever 1989). Even though Holothuroidea species alternate between unidirectional movement, a run-and-mill strategy and loops (Kaufmann and Smith 1997), recolonization based on movement alone can be expected within a year. Hence, the recovery period reported in this study (3 years for a partial recovery and >20 years for full recovery) are comparatively long, which warrants further consideration. Deposit-feeding Holothuroidea depend on organic compounds from the sediment (Amaro et al. 2010) and some species feed selectively on fresh organic detritus (FitzGeorge-Balfour et al. 2010) and pigment-rich organic matter (Hudson et al. 2005). Additionally, movement activity of Holothuroidea has been linked to their search for patchily-distributed high-quality organic resources, including fresh phytodetritus (Smith et al. 1997). Food conditions in the disturbance tracks are thought to be unfavourable due to a dilution of high-quality organic matter by the ploughing disturbance (e.g. protein concentrations half a year post-disturbance at undisturbed sites: 6.86 ± 3.59 g protein m^{-2} and at disturbed sites: 3.59 ± 1.53 g protein m^{-2}; Forschungsverbund Tiefsee-Umweltschutz, unpubl.). Hence, one would expect that Holothuroidea will respond to these poorer food conditions by active emigration out of the disturbance tracks, leaving their densities in the disturbance tracks reduced compared to the surrounding sediments (i.e. undisturbed and reference sites). So, even though Holothuroidea have the capacity to recolonize the disturbed area in due time, recolonization may lag behind due to unfavorable food conditions. We speculate that this may explain the relatively long recovery periods found in our study. However, holothurians also select for the finer sediment particle fraction (Khripounoff and Sibuet 1980) and therefore a change in the sediment particle size and composition in disturbance tracks could reduce the recolonization speed as well.

6.4 Outlook to deep-sea mining impacts

We found that Holothuroidea abundance, community composition and respiration activity recovered from a small-scale disturbance event in the Peru Basin on an annual to decadal scale. However, the results of this study cannot be directly extrapolated to mining scenarios, because they describe the recovery of one mobile conspicuous taxon and other taxonomic groups, especially those of sessile organisms, will have very different recovery rates. The recovery also occurred in a relatively lightly disturbed area of only 10.8 km^2, whereas a single mining operation will likely remove polymetallic nodules over an area between 300 to >1000 km^2(Smith et al. 2008; Levin et al. 2016). The type of disturbance examined here (sediment and nodules ploughing with little removal of the upper sediment) is also not representative of the actual disturbances, which will be associated with nodule and surface sediment removal (Thiel und Tiefsee-Umweltschutz 2001). Furthermore, the CCZ is a key target area for deep-sea mining and spans across a range of trophic settings, which may delay recovery, and potentially cumulative effects, such as overlapping mining plumes from nearby mining operations or climate change-related shifts in POC export fluxes (Levin et al. 2016; Sweetman et al. 2017; Yool et al. 2017) were not considered in this current study. Ultimately, to gain more knowledge about potential recovery rates of fauna after industrial-scale mining, a scientifically supported industrial test-mining operation in the CCZ is required, and all species of megafauna as well as all size classes of fauna should be monitored for several decades after resource extraction.

7. Acknowledgements

The research leading to these results has received funding from the European Union Seventh Framework Programme (FP7/2007-2013) under the MIDAS project, grant agreement n° 603418

418 and by the JPI Oceans – Ecological Aspects of Deep Sea Mining project under NWO-ALW
419 grant 856.14.002 and BMBF grant number 03F0707A-G. AG in part was funded by the RSF
420 grant 14-50-00095. The authors thank PI Antje Boetius, Felix Janssen, the scientific party, the
421 captain and crew of RV Sonne as well as the ROV Kiel 6000 team from Geomar (Kiel) for their
422 excellent support during cruise SO242-2. We thank the editor and two anonymous reviewers for
423 their comments that helped to improve a previous version of this manuscript.
424
425

8. Reference

Ahnert, A. and G. Schriever. 2001. Response of abyssal Copepoda Harpacticoida (Crustacea) and other meiobenthos to an artificial disturbance and its bearing on future mining for polymetallic nodules. Deep Sea Res. Part II **48**: 3779-3794.

Amaro, T., S. Bianchelli, D. S. Billett, M. Cunha, A. Pusceddu, and R. Danovaro. 2010. The trophic biology of the holothurian *Molpadia musculus*: implications for organic matter cycling and ecosystem functioning in a deep submarine canyon. Biogeosciences **7**: 2419-2432.

Amon, D. J., A. F. Ziegler, T. G. Dahlgren, A. G. Glover, A. Goineau, A. J. Gooday, H. Wiklund, and C. R. Smith. 2016. Insights into the abundance and diversity of abyssal megafauna in a polymetallic-nodule region in the eastern Clarion-Clipperton Zone. Sci. Rep. 6: 30492. doi: 10.1038/srep30492.

Bett, B. J., M. G. Malzone, B. E. Narayanaswamy, and B. D. Wigham. 2001. Temporal variability in phytodetritus and megabenthic activity at the seabed in the deep Northeast Atlantic. Limnol. Oceanogr. **50**: 349-368.

Billett, D. S., B. Bett, W. Reid, B. Boorman, and I. Priede. 2010. Long-term change in the abyssal NE Atlantic: The 'Amperima Event' revisited. Deep Sea Res. Part II **57**: 1406-1417.

Billett, D. S., B. Bett, A. Rice, M. Thurston, J. Galéron, M. Sibuet, and G. Wolff. 2001. Long-term change in the megabenthos of the Porcupine Abyssal Plain (NE Atlantic). Prog. Oceanogr. **50**: 325-348.

Bluhm, H. 2001. Re-establishment of an abyssal megabenthic community after experimental physical disturbance of the seafloor. Deep Sea Res. Part II **48**: 3841-3868.

Bluhm, H., and A. Gebruk. 1999. Holothuroidea (Echinodermata) of the Peru Basin-Ecological and Taxonomic Remarks Based on Underwater Images. Mar. Ecol. **20**: 167-195.

Bluhm, H., G. Schriever, and H. Thiel. 1995. Megabenthic recolonization in an experimentally disturbed abyssal manganese nodule area. Mar. Georesour. Geotec. **13**: 393-416.

Bluhm, H., and H. Thiel. 1996. Photographic and video surveys for large scale animal and seafloor surface charting aiming at ecological characterization of habitats and communities. Proceedings of the International Seminar on Deep Seabed Mining Technology. October 18-20, 1996. Peking, PR China: C15-C23.

Boetius, A. 2015. Cruise Report SO242/2: DISCOL revisited. JPI OCEANS Ecological Aspects of Deep-Sea Mining. Guayaquil: 28.08.2015 – Guayaquil: 01.10.2015.

461 Borowski, C. 2001. Physically disturbed deep-sea macrofauna in the Peru Basin, southeast
462 Pacific, revisited 7 years after the experimental impact. Deep Sea Res. Part II **48**: 3809-
463 3839.

464 Borowski, C., and H. Thiel. 1998. Deep-sea macrofaunal impacts of a large-scale physical
465 disturbance experiment in the Southeast Pacific. Deep Sea Res. Part II **45**: 55-81.

466 Brooke, S., M. Holmes, and C. Young. 2009. Sediment tolerance of two different
467 morphotypes of the deep-sea coral *Lophelia pertusa* from the Gulf of Mexico. Mar.
468 Ecol.-Prog. Ser. **390**: 137-144.

469 Canals, M., P. Puig, X. D. De Madron, S. Heussner, A. Palanques, and J. Fabres. 2006.
470 Flushing submarine canyons. Nature **444**: 354-357.

471 Clarke, K., and R. Warwick. 2001. Change in marine communities: an approach to statistical
472 analysis and interpretation, PRIMER-E.

473 Danovaro, R., M. Fabiano, G. Albertelli, and N. D. Croce. 1995. Vertical distribution of
474 meiobenthos in bathyal sediments of the eastern Mediterranean Sea: relationship with
475 labile organic matter and bacterial biomasses. Mar. Ecol. **16**: 103-116.

476 Danovaro, R., M. Fabiano, and N. Della Croce. 1993. Labile organic matter and microbial
477 biomasses in deep-sea sediments (Eastern Mediterranean Sea). Deep Sea Res. Part I **40**:
478 953-965.

479 De Leo, F. C., C. R. Smith, A. A. Rowden, D. A. Bowden, and M. R. Clark. 2010. Submarine
480 canyons: hotspots of benthic biomass and productivity in the deep sea. Proc. R. Soc. B
481 **277**: 2783–2792.

482 Dunlop, K. M., D. van Oevelen, H. A. Ruhl, C. L. Huffard, L. A. Kuhnz, and K. L. Smith.
483 2016. Carbon cycling in the deep eastern North Pacific benthic food web: Investigating
484 the effect of organic carbon input. Limnol. Oceanogr. **61**: 1956-1968.

485 Durden, J. M., and others. 2016. Perspectives in visual imaging for marine biology and
486 ecology: from acquisition to understanding. Oceanogr. Mar. Biol. **54**: 1-72.

487 Fitzgeorge-Balfour, T., D. S. Billett, G. A. Wolff, A. Thompson, and P. A. Tyler. 2010.
488 Phytopigments as biomarkers of selectivity in abyssal holothurians; interspecific
489 differences in response to a changing food supply. Deep Sea Res. Part II **57**: 1418-1428.

490 Foell, E., H. Thiel, and G. Schriever. 1990. DISCOL: A long-term, large-scale, disturbance-
491 recolonization experiment in the abyssal eastern tropical South Pacific Ocean. Offshore
492 Technology Conference, 1990.

493 Foell, E., H. Thiel, and G. Schriever. 1992. DISCOL: a long-term, large-scale, disturbance-
494 recolonization experiment in the abyssal eastern tropical South Pacific Ocean. Min. Eng.
495 **44**: 90-94.

Glasby, G. 2000. Lessons learned from deep-sea mining. Science **289**: 551-553.

Gollner, S., S. Kaiser, L. Menzel, D. O. Jones, A. Brown, N. C. Mestre, D. van Oevelen, L. Menot, A. Colaço, and M. Canals. 2017. Resilience of benthic deep-sea fauna to mining activities. Mar. Environ. Res. **129**: 76-101.

Greinert, J. 2015. Cruise Report SO242/1: JPI OCEANS Ecological Aspects of Deep-Sea Mining. DISCOL Revisited. Guayaquil: 27.07.2015 – Guayaquil: 25.08.2015. GEOMAR Helmholtz-Zentrum für Ozeanforschung Kiel.

Gruppe, B., H. J. Becker, and H. U. Oebius. 2001. Geotechnical and sedimentological investigations of deep-sea sediments from a manganese nodule field of the Peru Basin. Deep Sea Res. Part II **48**: 3593-3608.

Haeckel, M., I. König, V. Riech, M. E. Weber, and E. Suess. 2001. Pore water profiles and numerical modelling of biogeochemical processes in Peru Basin deep-sea sediments. Deep Sea Res. Part II **48**: 3713-3736.

Hudson, I. R., B. D. Wigham, and P. A. Tyler. 2004. The feeding behaviour of a deep-sea holothurian, *Stichopus tremulus* (Gunnerus) based on in situ observations and experiments using a Remotely Operated Vehicle. J. Exp. Mar. Biol. and Ecol. **301**: 75-91.

Hughes, S. J. M., H. A. Ruhl, L. E. Hawkins, C. Hauton, B. Boorman, and D. S. Billett. 2011. Deep-sea echinoderm oxygen consumption rates and an interclass comparison of metabolic rates in Asteroidea, Crinoidea, Echinoidea, Holothuroidea and Ophiuroidea. J. Exp. Biol. **214**: 2512-2521.

Jamieson, A. J., A. Gebruk, T. Fujii, and M. Solan. 2011. Functional effects of the hadal sea cucumber Elpidia atakama (Echinodermata: Holothuroidea, Elasipodida) reflect small-scale patterns of resource availability. Mar. Biol. **158**: 2695-2703.

Jankowski, J. A., and W. Zielke. 2001. The mesoscale sediment transport due to technical activities in the deep sea. Deep Sea Res. Part II **48**: 3487-3521.

Jones, D. O. B., and others. 2017. Biological responses to disturbance from simulated deep-sea polymetallic nodule mining. PloS One **12**: e0171750. doi:10.1371/journal.pone.0171750.

Kaufmann, R., and K. Smith. 1997. Activity patterns of mobile epibenthic megafauna at an abyssal site in the eastern North Pacific: results from a 17-month time-lapse photographic study. Deep Sea Res. Part I **44**: 559-579.

Khripounoff, A., J.-C. Caprais, P. Crassous, and J. Etoubleau. 2006. Geochemical and biological recovery of the disturbed seafloor in polymetallic nodule fields of the Clipperton-Clarion Fracture Zone (CCFZ) at 5,000-m depth. Limnol. Oceanogr. **51**: 2033-2041.

Khripounoff, A, and M. Sibuet. 1980. La nutrition d'echinodermes abyssaux. I. Alimentation des holothuries. Mar. Biol. **60**: 17-26.

Klein, G., E. Rachor, and S. A. Gerlach. 1975. Dynamics and productivity of two populations of the benthic tube-dwelling amphipod *Ampelisca brevicornis* (Costa) in Helgoland Bight. Ophelia **14**: 139-159.

Levin, L. A., and others. 2016. Defining "serious harm" to the marine environment in the context of deep-seabed mining. Mar. Policy **74**: 245-259.

Linke, P. 2010. Cruise Report SO-210: ChiFlux. Identification and investigation of fluid flux, mass wasting and sediments in the forearc of the central Chilean subduction zone. Valparaiso: 23.09.2010 – Valparaiso: 01.11.2010. GEOMAR Helmholtz-Zentrum für Ozeanforschung Kiel.

Lopez-Fernandez, P., S. Bianchelli, A. Pusceddu, A. Calafat, R. Danovaro, and M. Canals. 2013a. Bioavailable compounds in sinking particulate organic matter, Blanes Canyon, NW Mediterranean Sea: effects of a large storm and sea surface biological processes. Prog. Oceanogr. **118**: 108-121.

Lopez-Fernandez, P., S. Bianchelli, A. Pusceddu, A. Calafat, A. Sanchez-Vidal, and R. Danovaro. 2013b. Bioavailability of sinking organic matter in the Blanes canyon and the adjacent open slope (NW Mediterranean Sea). Biogeosciences **10**: 3405-3420.

Magurran, A. E. 2004. Measuring biological diversity, Blackwell Science Ltd.

Marchig, V., U. von Stackelberg, H. Hufnagel, and G. Durn. 2001. Compositional changes of surface sediments and variability of manganese nodules in the Peru Basin. Deep Sea Res. Part II **48**: 3523-3547.

Marcon, Y. and A. Purser. 2017. PAPARA (ZZ) I: An open-source software interface for annotating photographs of the deep-sea. SoftwareX **6**: 69-80.

Miller, J. E., and D. L. Pawson. 1990. Swimming sea cucumbers (Echinodermata: Holothuroidea): a survey, with analysis of swimming behavior in four bathyal species. Smithson. Contrib. Mar. Sci. **35**: 1-18.

Leitner, A. B., A. Neuheimer, E. Donlon, C. R. Smith, and J. C. Drazen. 2016. Environmental and Bathymetric Influences on Abyssal Bait-Attending Communities of the Clarion Clipperton Zone, Deep Sea Res. Part I **125**: 65-80.

Oebius, H. U., H. J. Becker, S. Rolinski, and J. A. Jankowski. 2001. Parameterization and evaluation of marine environmental impacts produced by deep-sea manganese nodule mining. Deep Sea Res. Part II **48**: 3453-3467.

Oksanen, J., F. G., and others. 2017. vegan: Community Ecology Package. R package version 2.4-3. URL: https://CRAN.R-project.org/package=vegan.

566 Purser, A., Y. Marcon, H.-J. T. Hoving, M. Vecchione, U. Piatkowski, D. Eason, H. Bluhm,
567 and A. Boetius. 2016. Association of deep-sea incirrate octopods with manganese crusts
568 and nodule fields in the Pacific Ocean. Curr. Biol. **26**: R1247–R1271.

569 R Core Team. 2016. R: A language and environment for statistical computing. R Foundation
570 for Statistical Computing, Vienna, Austria. URL: https://www.R-project.org/.

571 Rogacheva, A., A. Gebruk, and C. H. Alt. 2012. Swimming deep-sea holothurians
572 (Echinodermata: Holothuroidea) on the northern Mid-Atlantic Ridge. Zoosymposia **7**:
573 213-224.

574 Ruhl, H. A. 2007. Abundance and size distribution dynamics of abyssal epibenthic megafauna
575 in the northeast Pacific. Ecology **88**: 1250-1262.

576 Ruhl, H. A., B. J. Bett, S. J. M. Hughes, C. H. Alt, E. J. Ross, R. S. Lampitt, C. A. Pebody, K.
577 L. Smith, and D. S. Smith. 2014. Links between deep-sea respiration and community
578 dynamics. Ecology **95**: 1651-1662.

579 Schriever, G., Koschinsky, A, and H. Bluhm. 1996. Cruise Report ATESEPP. Auswirkungen
580 technischer Eingriffe in das Ökosystem der Tiefsee im Süd-Ost-Pazifik vor Peru.
581 (Impacts of potential technical interventions on the deep-sea ecosystem of the southeast
582 Pacific off Peru). Sonne Cruise 106. January 1 – March 9, 1996 Balboa/ Panama –
583 Balboa/ Panama. Berichte aus dem Zentrum für Meeres- und Klimaforschung. Reihe E:
584 Hydrobiologie und Fischereiwissenschaft Nr. 11. Institut für Hydrobiologie und
585 Fischereiwissenschaft Hamburg.

586 Smallwood, B. J., G. A. Wolff, B. J. Bett, C. R. Smith, D. Hoover, J. D. Gage, and A.
587 Patience. 1999. Megafauna can control the quality of organic matter in marine sediments.
588 Naturwissenschaften 86: 320-324.

589 Smith, A., J. Matthiopoulos, and I. G. Priede. 1997. Areal coverage of the ocean floor by the
590 deep-sea elasipodid holothurian *Oneirophanta mutabilis*: estimates using systematic,
591 random and directional search strategy simulations. Deep Sea Res. Part I **44**: 477-486.

592 Smith, C. R., L. A. Levin, A. Koslow, P. A. Tyler, and A. G. Glover. 2008, 334-352 The near
593 future of the deep seafloor ecosystem. In: N. Polunin [ed.], Aquatic Ecosystems: Trends
594 and Global Prospects. Cambridge University Press.

595 Smith, K. L., R. Kaufmann, and W. Wakefield. 1993. Mobile megafaunal activity monitored
596 with a time-lapse camera in the abyssal North Pacific. Deep Sea Res. Part I **40**: 2307-
597 2324.

598 Sweetman, A. K., and others. 2017. Major impacts of climate change on deep-sea benthic
599 ecosystems. Elementa - Science of the Anthropocene **5**: 4. doi: 10.1525/elementa.203.

600 Thiel, H., and G. Schriever. 1989. Cruise Report SO61. DISCOL 1. Balboa; 02.02.1989 –
601 Callao: 03.04.1989. Zentrum für Meeres- und Klimaforschung der Universität Hamburg.
602 Institut für Hydrobiologie und Fischereiwissenschaft.

Thiel, H., and Forschungsverbund Tiefsee-Umweltschutz. 2001. Evaluation of the environmental consequences of polymetallic nodule mining based on the results of the TUSCH Research Association. Deep Sea Res. Part II **48**: 3433-3452.

Thurber, A. R., A. K. Sweetman, B. E. Narayanaswamy, D. O. B. Jones, J. Ingels, and R. L. Hansman. 2014. Ecosystem function and services provided by the deep sea. Biogeosciences **11**: 3941-3963.

van Oevelen, D., K. Soetaert, R. García, H. de Stigter, M. R. Cunha, A. Pusceddu, and R. Danovaro. 2011. Canyon conditions impact carbon flows in food webs of three sections of the Nazaré canyon. Deep Sea Res. Part II **58**: 2461-2476.

Vanreusel, A., A. Hilario, P. A. Ribeiro, L. Menot, and P. Martinez Arbizu. 2016. Threatened by mining, polymetallic noduels are required to preserve abyssal epifauna. Sci. Rep. **6**: 26808. doi: 10.1038/srep26808.

Wang, X., and W. E. Müller. 2009. Marine biominerals: perspectives and challenges for polymetallic nodules and crusts. Trends Biotechnol. **27**: 375-383.

Wiedicke, M. H., and E. M. Weber. 1996. Small-scale variability of seafloor features in the northern Peru Basin: Results from acoustic survey methods. Mar. Geophys. Res. **18**: 507-526.

Yool, A., A. P. Martin, T. R. Anderson, B. J. Bett, D. O. Jones, and H. A. Ruhl. 2017. Big in the benthos: Future change of seafloor community biomass in a global, body size-resolved model. Glob. Change Biol. **00**:1–13. doi:10.1111/gcb.13680.

625 **Table 1:** Ocean floor observation system (OFOS) transects. For each disturbance level
626 (undisturbed, disturbed, and reference) photos of four OFOS transects were analyzed (Ref S =
627 reference south; Ref SE = reference southeast; Dist. = disturbed within DEA; Undist. =
628 undisturbed within DEA). As both disturbed and undisturbed within DEA photo sets originate
629 from the same bottom tracks, the only difference between the photos was the presence of visible
630 plough marks in the images.
631

OFOS transect	**Start of bottom transect**	**End of bottom transect**	**Usable photos**	**Seafloor area imaged (m^2)**	**Disturbance level**
139	7°07.71'S, 8°826.92'W	7°07.24'S, 8°827.16'W	87	418.0	Ref S
184	7°07.65'S, 8°827.20'W	7°06.86'S, 8°827.01'W	408	2069.0	Ref S
195	7°07.49'S, 8°827.00'W	7°06.98'S, 8°826.22'W	494	3015.7	Ref S
220	7°07.75'S, 8°825.96'W	7°05.76'S, 8°824.83'W	983	5434.7	Ref SE
155	7°04.50'S, 8°828.74'W	7°04.35'S, 8°827.36'W	498	2901.5	Dist.
212	7°05.57'S, 8°827.42'W	7°03.57'S, 8°827.46'W	792	390.4	Dist.
223	7°04.81'S, 8°828.21'W	7°05.06'S, 8°826.67'W	156	797.4	Dist.

227	7°04.65’S, 8°827.99’W	7°04.60’S, 8°826.36’W	392	1957.7	Dist.
155	7°04.50’S, 8°828.74’W	7°04.35’S, 8°827.25’W	338	2062.5	Undist.
212	7°05.57’S, 8°827.42’W	7°03.58’S, 8°827.45’W	473	2439.5	Undist.
223	7°04.80’S, 8°828.21’W	7°05.07’S, 8°826.71’W	676	3610.7	Undist.
227	7°04.63’S, 8°828.16’W	7°04.60’S, 8°826.33’W	435	2508.0	Undist.

632

633

634 **Table 2:** Density (ind. ha^{-1}) and respiration ($\times 10^{-3}$ mmol C m^{-2} d^{-1}) of the three most abundant

635 Holothuroidea taxa for each location (Ref S = reference south; Ref SE = reference southeast;

636 Dist. = disturbed within DEA; Undist. = undisturbed within DEA).

637

OFOS transect	Disturbance level	*Benthodytes typica*		*Amperima* sp.		*Mesothuria* sp.	
		Density	Respiration	Density	Respiration	Density	Respiration
139	Ref S	Not seen		52	0.22	52	0.06
184	Ref S	34	0.14	25	0.07	49	0.05
195	Ref S	47	0.27	41	0.12	41	0.05
220	Ref SE	38	0.29	15	0.06	22	0.04
155	Dist.	28	0.20	25	0.08	35	0.02
212	Dist.	62	0.43	28	0.11	26	0.03
223	Dist.	25	0.16	50	0.22	25	0.46
227	Dist.	97	0.63	26	0.11	31	0.06
155	Undist.	20	0.09	66	0.32	25	0.05
212	Undist.	70	0.33	50	0.29	41	0.07
223	Undist.	36	0.26	25	0.13	25	0.07
227	Undist.	53	0.43	18	0.10	26	0.06

638

639 **Table 3:** Holothuroidea density (ind. ha^{-1}), respiration ($\times 10^{-3}$ mmol C m^{-2} d^{-1}) and density based
640 diversity metrics (H': Shannon Index; J': Pielou's evenness) for each location (Ref S = reference
641 south; Ref SE = reference southeast; Dist. = disturbed within DEA; Undist. = undisturbed within
642 DEA).

643

OFOS transect	Disturbance level	Density	Respiration	H'	J'
139	Ref S	261	0.60	1.89	0.59
184	Ref S	230	0.46	2.30	0.72
195	Ref S	274	0.66	2.33	0.73
220	Ref SE	200	0.62	2.00	0.63
Mean ± sd	Ref	241±33	0.58±0.09	2.13±0.22	0.67±0.07
155	Dist.	183	0.45	2.38	0.75
212	Dist.	293	1.04	2.69	0.85
223	Dist.	214	0.66	2.07	0.65
227	Dist.	272	1.06	2.19	0.69
Mean ± sd	Dist.	241±51	0.80±0.30	2.33±0.27	0.74±0.09
155	Undist.	233	0.71	2.30	0.72
212	Undist.	297	0.92	2.44	0.77
223	Undist.	226	0.74	2.60	0.82
227	Undist.	203	0.73	2.34	0.74
Mean ± sd	Undist.	240±40	0.77±0.10	2.42±0.13	0.76±0.04

644

Figure captions

Figure 1. A) Map of the Peru Basin with bottom transects of all ocean floor observation system (OFOS) deployments inside the DISCOL experimental area (DEA, yellow circle) and at the southern and southeastern reference site. The number on white background correspond to the site numbers in Tab. 1. The black rectangle in the inserted map shows the exact location of DEA, but is unscaled. B) Photograph of plough marks in the sediment at the DISCOL experimental area. C) Photograph of seafloor at the reference site.

Figure 2. Images of Holothuroidea morphotypes used in the present study: A. *Abyssocucumis abyssorum,* B. *Elpidiidae* gen. sp.1 [= *Achlyoinice* sp. in Bluhm and Gebruk (1999)], C. *Amperima* sp., D. *Benthodytes gosarsi,* E. *Benthodytes* sp., F. *Benthodytes typica,* G. Elp_sp2 = *Elpidiidae* gen. sp. 2 ("double velum" morphotype in ccfzatlas.com), H. *Elpidiidae* gen. sp. 3, I. *Benthothuria* sp., J. *Mesothuria* sp., K. *Oneirophanta* sp., L. *Galatheathuria* sp., M. *Peniagone* sp. (= morphotype "palmata" in ccfzatlas.com), N. *Peniagone* sp.1, O. *Peniagone* sp. 2 (benthopelagic), P. *Psychronaetes hanseni,* Q. *Psychropotes depressa,* R. *Psychropotes longicauda,* S. *Bathyplotes* sp., T. *Synallactidae* gen. sp. 1, U. *Synallactidae* gen. sp. 2, V. *Synallactes profundi,* W. *Synallactes* sp. (morphotype "pink" in ccfzatlas.com).
The black bar represents 1 cm length. Photographs A, C- F, I, K- M, P-W from AWI; B, G, J, N from ROV Kiel 6000, Geomar; H, O from T. Stratmann.

Figure 3. Holothuroidea morphotype densities >60 ind. ha^{-1} (A), >40 ind. ha^{-1} (B) and >10 ind. ha^{-1} (C) in the three areas disturbed within DEA, undisturbed within DEA, and reference, shown as mean values with standard deviations.

Abbreviations are: Aby_aby = *Abyssocucumis abyssorum*, Amp_sp. = *Amperima* sp., Bath_sp. = *Bathyplotes* sp., Ben_gos = *Benthodytes gosarsi*, Ben_sp. = *Benthodytes* sp., Ben_typ = *Benthodytes typica*, Beu_sp. = *Benthothuria* sp., Elp_sp1 = Elpidiidae gen. sp. 1 [= *Achlyoinice* sp. in Bluhm and Gebruk (1999)], Elp_sp2 = *Elpidiidae* gen. sp. 2 ("double velum" morphotype in ccfzatlas.com), Elp_sp3 = *Elpidiidae* gen. sp. 3, Gal_sp. = *Galatheathuria* sp., Mes_sp. = *Mesothuria* sp., One_sp. = *Oneirophanta* sp., Pen_pal = *Peniagone* sp. (= morphotype "palmate" in ccfzatlas.com), Pen_sp1 = *Peniagone* sp. 1, Pen_swi = *Peniagone* sp. 2 (benthopelagic), Pse_han = *Psychronaetes hanseni*, Psy_dep = *Psychropotes depressa*, Psy_lon = *Psychropotes longicauda*, Syn_pin = *Synallactes* sp. (morphotype "pink" in ccfzatlas.com), Syn_pro = *Synallactes profundi*, Syn_sp1 = *Synallactidae* gen. sp. 1, Syn_sp2 = *Synallactidae* gen. sp. 2, Unknown = Unknown Holothurian.

Figure 4. Holothuroidea densities measured during all previous post-disturbance DISCOL cruises at the disturbed as well as undisturbed sites, and, pre- and post-impact in the reference areas (no data were available for the cruise 0.1 years after ploughing). Data from pre-disturbance (-0.1 years), 0.1 years, 0.5 years, 3 years and 7 years after the DISCOL experiment were taken from Bluhm (2001) annex 2.08. n. d. means that no data were available for this specific disturbance and year (disturbed and undisturbed site at -0.1 years; reference at 0.1 years).

686 Figure 1

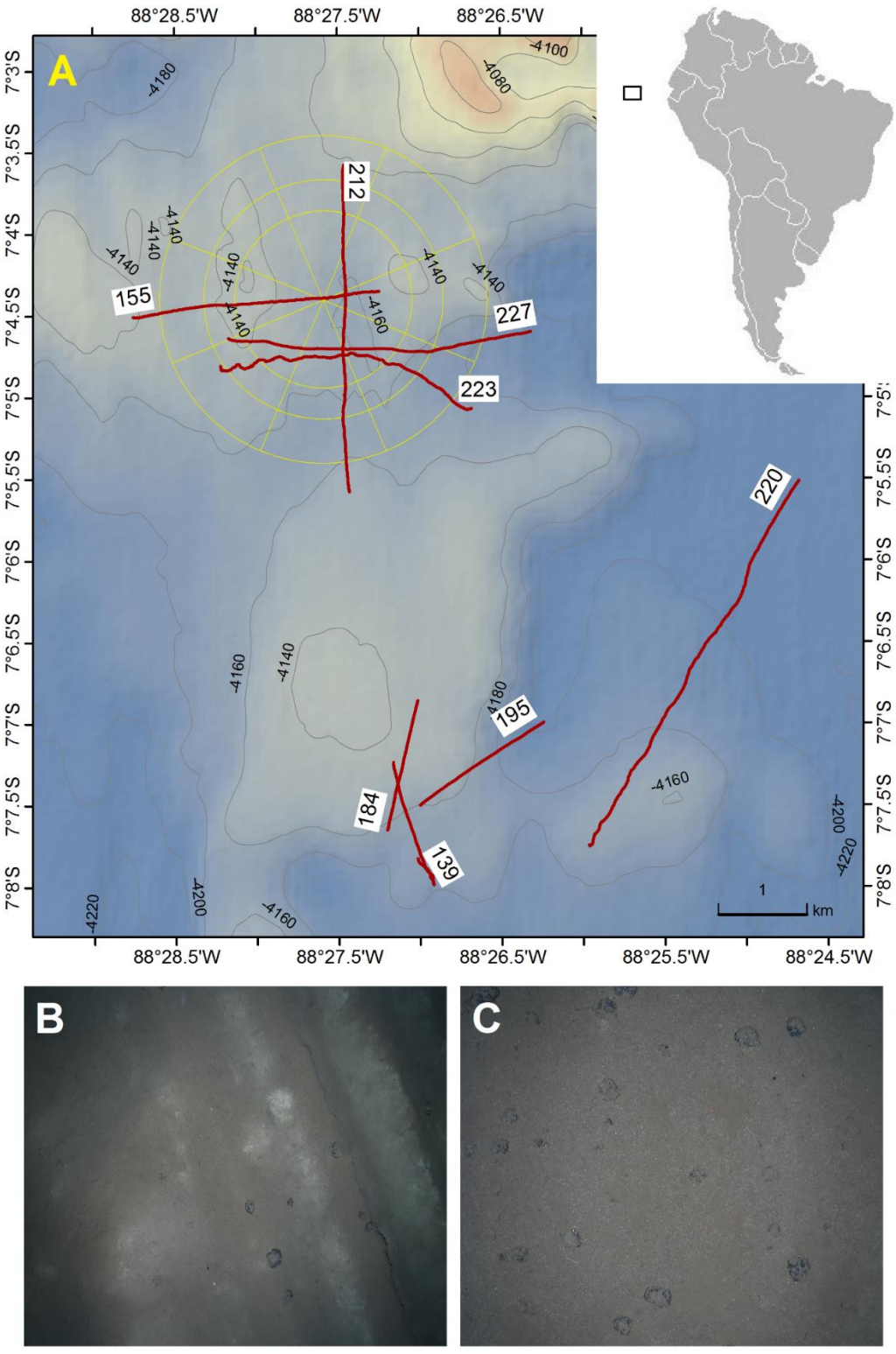

687

688 Figure 2

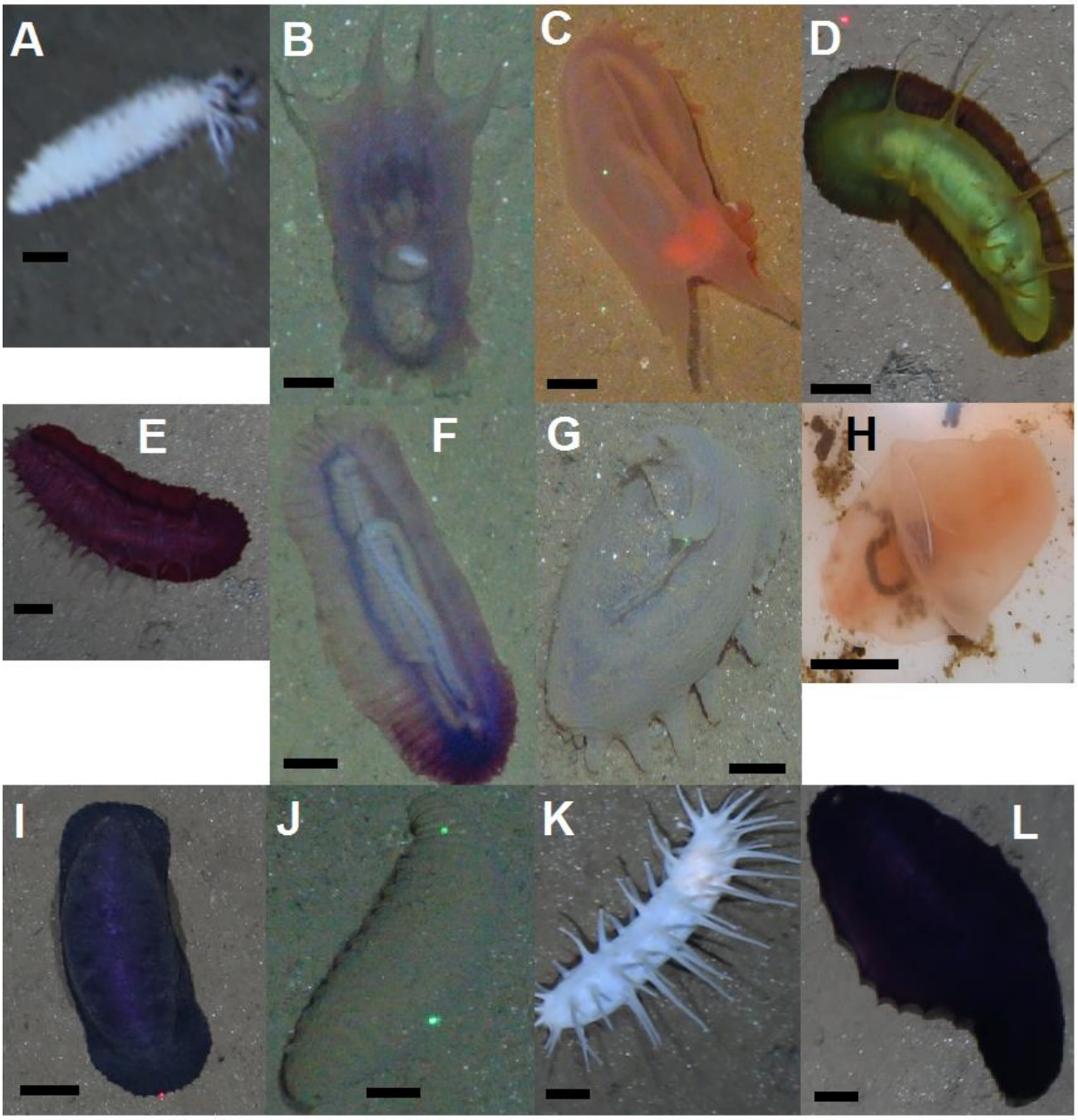

689

690

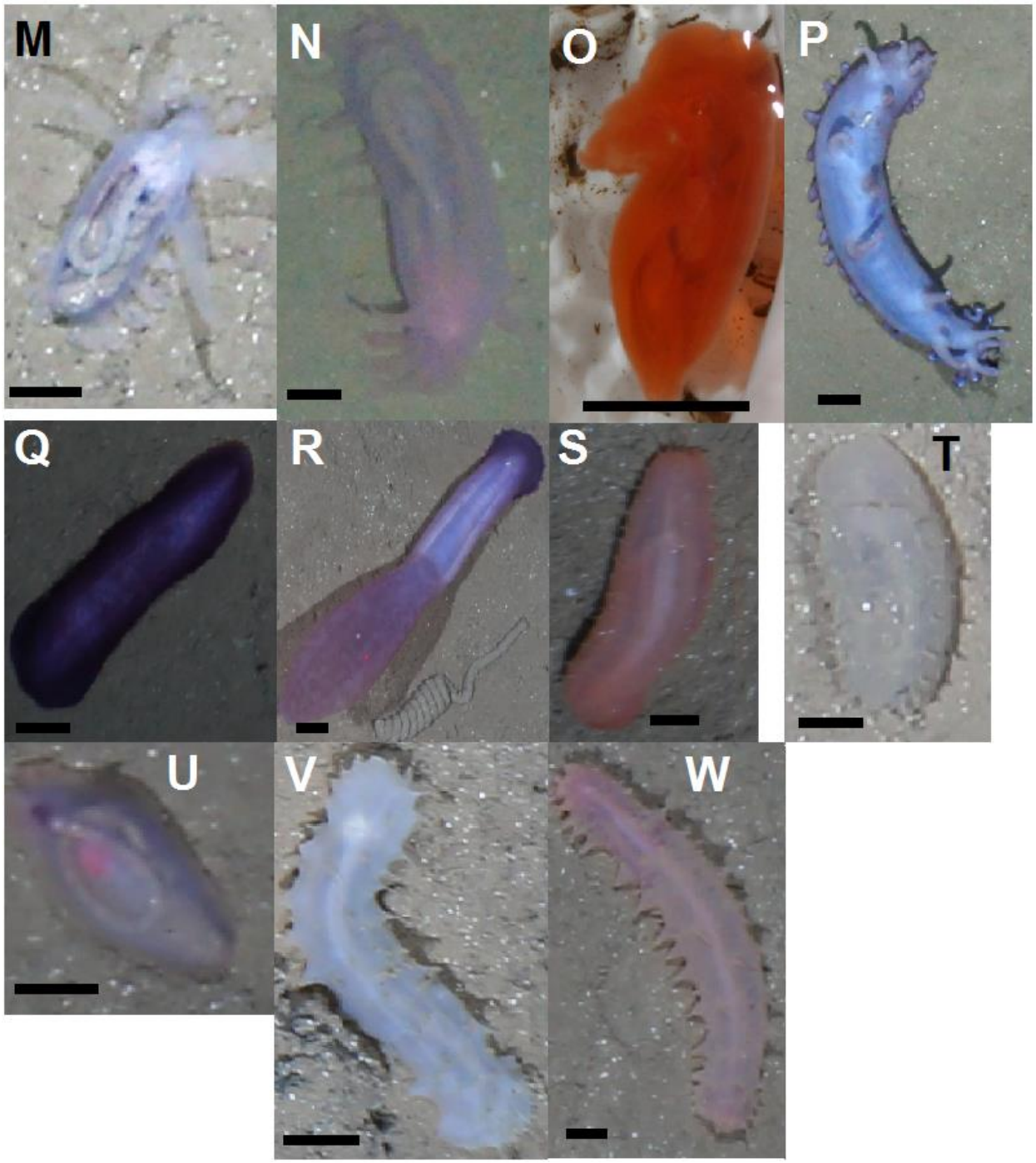

691

Figure 3

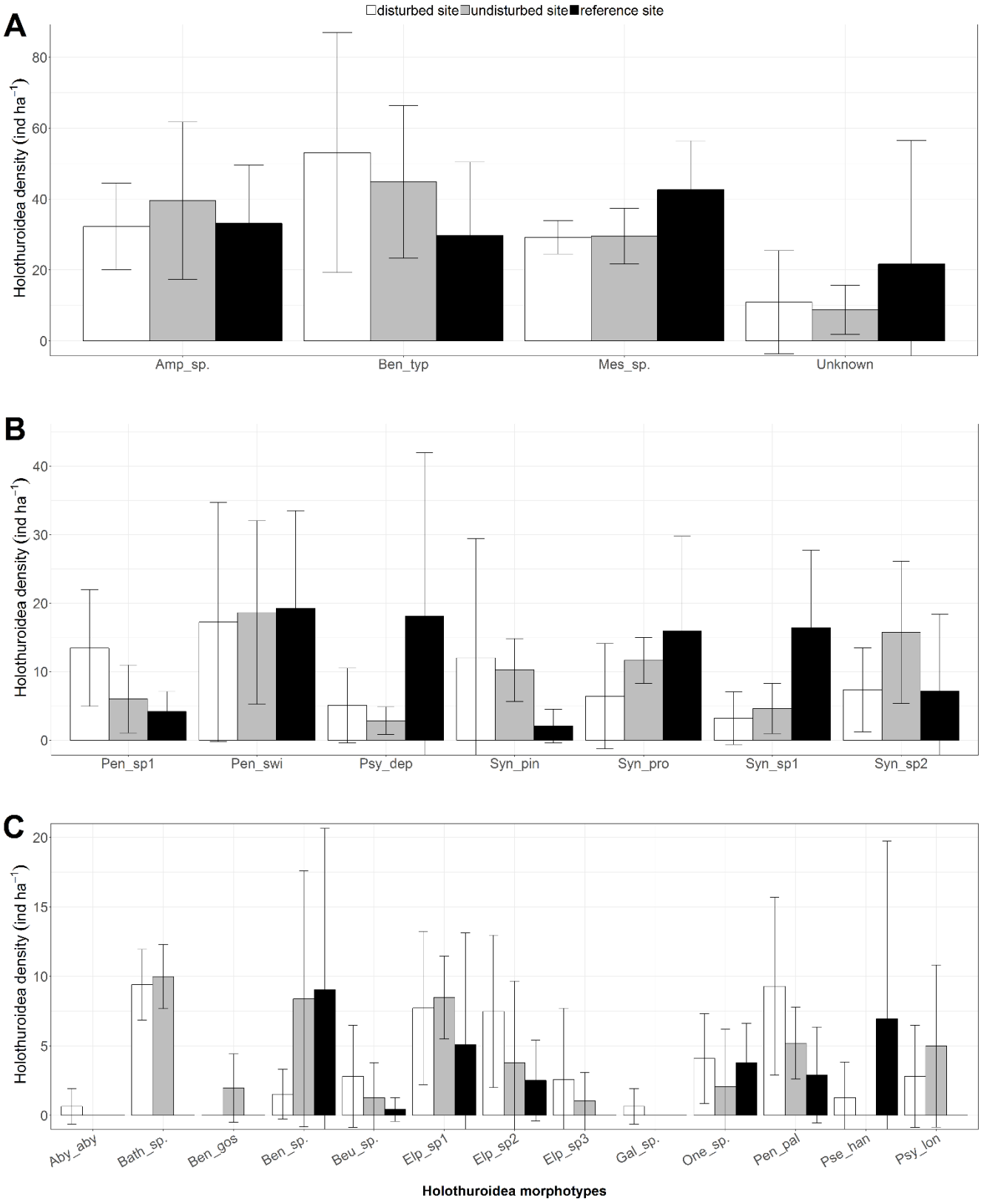
disturbed site
undisturbed site
reference site
A
Holothuroidea density (ind ha^{-1})
0
20
40
60
80
Amp_sp.
Ben_typ
Mes_sp.
Unknown
B
Holothuroidea density (ind ha^{-1})
0
10
20
30
40
Pen_sp1
Pen_swi
Psy_dep
Syn_pin
Syn_pro
Syn_sp1
Syn_sp2
C
Holothuroidea density (ind ha^{-1})
0
5
10
15
20
Aby_aby
Bath_sp.
Ben_gos
Ben_sp.
Beu_sp.
Elp_sp1
Elp_sp2
Elp_sp3
Gal_sp.
One_sp.
Pen_pal
Pse_han
Psy_lon
Holothuroidea morphotypes

Figure 4

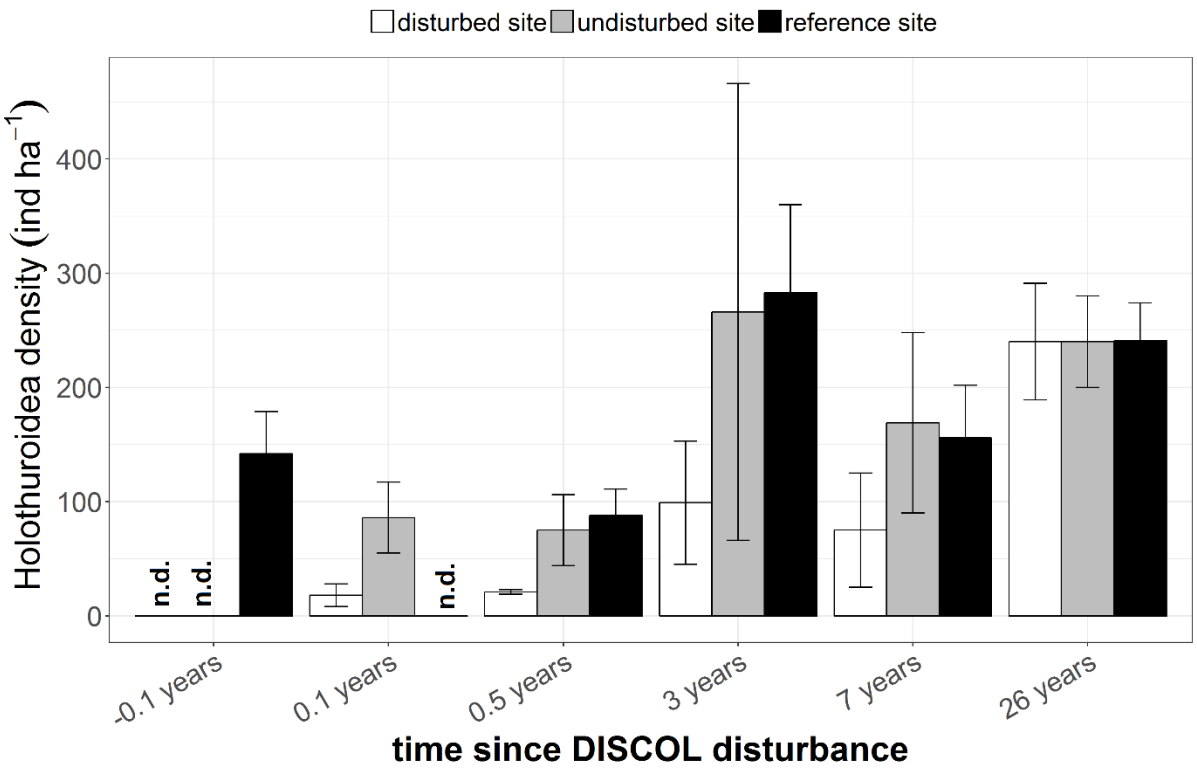
disturbed site
undisturbed site
reference site
Holothuroidea density (ind ha^{-1})
400
300
200
100
0
n.d.
n.d.
n.d.
-0.1 years
0.1 years
0.5 years
3 years
7 years
26 years
time since DISCOL disturbance